論文内容の要旨

論文題目：Structure and Formation Mechanism of Lead Perovskite Crystals
（鉛ペロブスカイト結晶の構造と形成機構）

氏名　庄山 和隆

1. Introduction

The process of assembling elements into useful materials is a fascinating moment for materials scientists. In this thesis is presented mechanistic insight of a material formatting process that involves a crystal-to-crystal conversion reaction to yield a crystalline material, and related studies on the crystallographic properties of it. Specifically I will focus on methylammonium lead triiodide ($CH_3NH_3^+PbI_3^-$; $MA^+PbI_3^-$; **PV**), which is in the last few years extensively studied for solar cell application. This material has one of the commonest mineral structures, the perovskite crystal structure, and is attractive due to superior performance of devices using it, thus deserves as an example of crystal-to-crystal conversion reactions.

The most important subject in this study is how the three-dimensional (3-D) cubic structure of **PV** forms from the two-dimensional (2-D) sheet structure of lead(II) iodide (PbI_2; **PI**) in the presence of methylammonium iodide (MAI) and a polar solvent (*N*,*N*-dimethylformamide; DMF or dimethylsulfoxide; DMSO). It was found that the pathways from **PI** to **PV** are in equilibrium connected by one-dimensional (1-D) multi-nuclear strips of plumbate(II). This equilibrium involves reversible participation of the solvent as studied by *in situ* XRD measurements of free-standing fibrous intermediates isolated from precursor solutions prepared in a similar manner as the fabrication process of solar cells. The detailed kinetic study showed two detrimental roles of the solvent molecules, which are to exfoliate the layered 2-D structure of **PI** to form the 1-D structure of intermediates and to facilitate the inter-conversion between the 1-D structure of intermediates and the 3-D structure of **PV**.

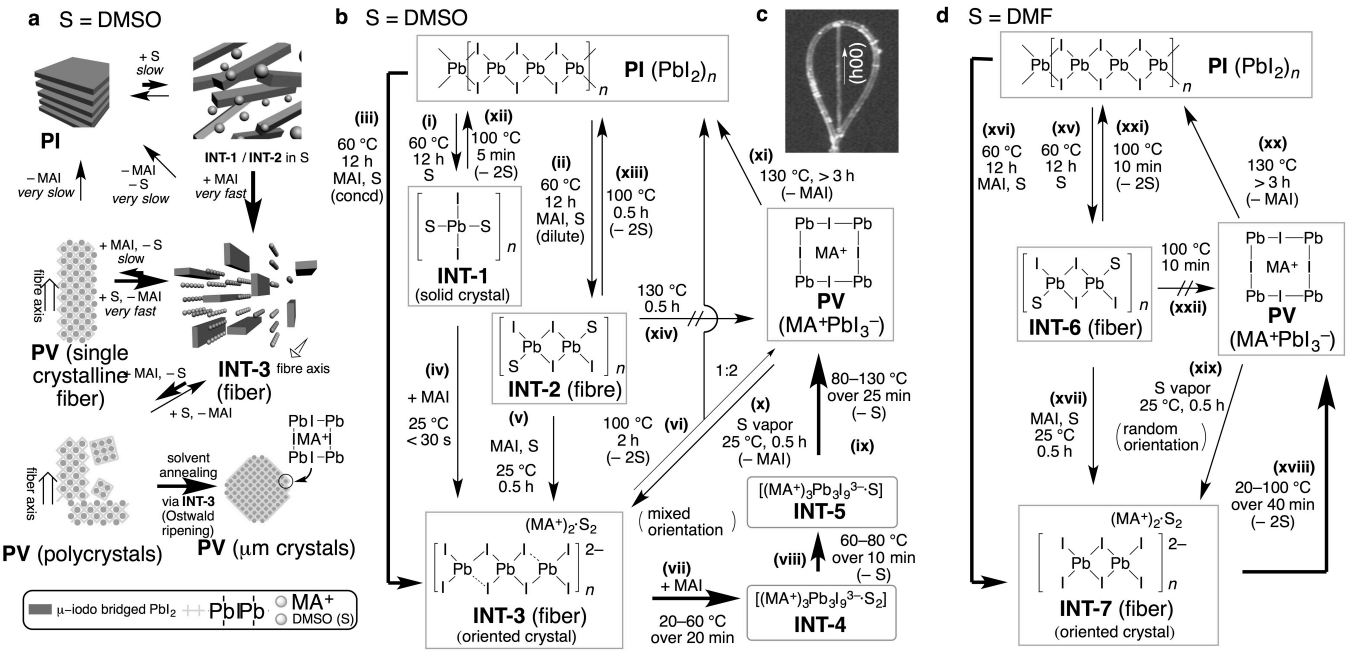

Figure 1. The chemical pathways involved in the formation of **PV**. (a) Schematic image of the inter-conversion between **PI** and **PV** in DMSO system. (b) Chemical structures and each process of DMSO system. (c) Optical image of **INT-3**. (d) Chemical structures and each process of DMF system.

2. Results and discussion

2.1 The chemical equilibrium of a system comprise PI, MAI, and solvent

The fibrous intermediates were isolated in polar solvents, namely DMF and DMSO, which are used in almost all cases of solution-processed perovskite solar cell fabrication. Several of them were already characterized; others were reported here for the first time. The DMF case is simper thus explained first. Mixing 1 to 1 mole ratio of MAI and **PI** in DMF at 60 °C for 12 h yielded a yellow solution, which upon cooling to room temperature formed fibrous precipitates of di-nuclear strips of iodine-coordinated plumbate(II) ($(MA^+)_2(PbI_3^-)_2{\cdot}DMF_2$; **INT-7**). This plumbate **INT-7** was also prepared in two steps via simple di-nuclear strips of plumbate(II) ($(PbI_2)_2{\cdot}DMF_2$; **INT-6**). The fibrous plumbate **INT-7** converted to **PV** by heating to 100 °C, maintaining the fibrous structure. Treating the fibrous **PV** by DMF vapor reverted it to **INT-7**, demonstrating the thermodynamic stability of **INT-7** against other chemical species in the system comprise **PI**, MAI, and DMF. When the fibrous **PV** was heated to 130 °C over 3 h it started to decompose to **PI**. A similar picture of the processes in the system was observed for the DMSO case, with a few important exceptions. First of all, the thermodynamically most stable species was not di-nuclear strips of plumbate but tri-nuclear strips of a mixture of iodine-coordinated and simple plumbate(II) ($(MA^+)_2[(PbI_3^-)_2(PbI_2)]{\cdot}DMSO_2$; **INT-3**). Secondly in the two-step preparation of the plumbate **INT-3** were two kinds of plumbate(II), namely mono-nuclear strips ($PbI_2{\cdot}DMSO_2$; **INT-1**) and di-nuclear strips ($(PbI_2)_2{\cdot}DMSO_2$; **INT-2**). Thirdly, the conversion of **INT-3** to **PV** required the coating of its surface with MAI as suggested by the stoichiometric insufficiency of MAI; otherwise it produced a mixture of PI and PV. Lastly, during the conversion of **INT-3** to **PV** there were two additional intermediates (**INT-4** and **INT-5**), which were characterized by 2-D diffraction images of the *in situ* XRD measurements (*vide infra*).

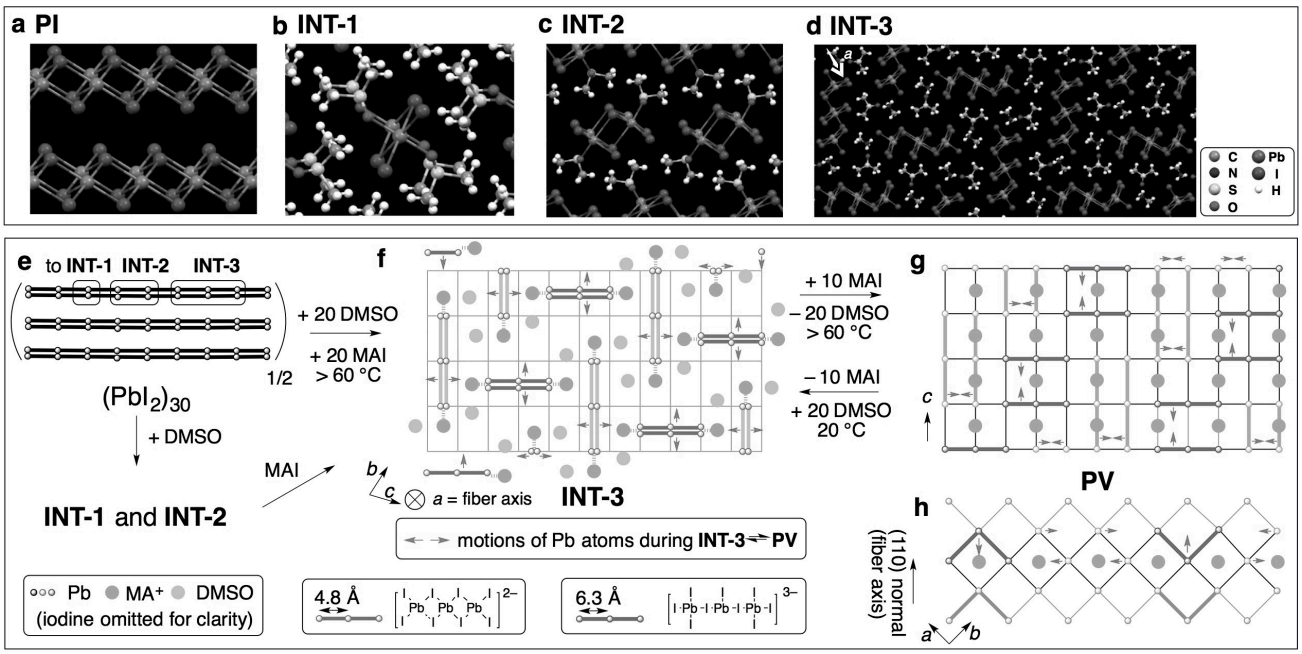

Figure 2. Crystal structures of **PI** and intermediates, and topological correlation between **PI**–**INT-3**-**PV** in DMSO system. (a) Crystal structure of **PI**. (b) **INT-1**. (c) **INT-2**. (d) **INT-3**. (e) Topological image of two layers of **PI**. (f) **INT-3**. (g) **PV** from top of the fiber axis. (h) Front view of Fig. 2g.

2.2 The structural correlation between the 1-D plumbate(II) and 3-D perovskite

The facile inter-conversion between the 1-D strips of plumbate(II) and 3-D cubic perovskite structure suggests their structural correlation. As discussed later two of the crystallographic cubic axes of the perovskite fibers prepared from **INT-3** are inclined by 45° against the fiber axis of **INT-3**. This information allows atom displacement mapping between **INT-3** and **PV** during the conversion. Thus as shown in Fig. 2f, seen from the top of the fiber axis, the truncated plumbate structure of **PI** can be placed on the grid of the cubic lattice of **PV**. The atom movements can also be mapped as displayed in the inter-conversion in Fig. 2f, g. The tri-nuclear plumbate strips depart one another to form two columns along the fiber axis. At the same time one of the lead atoms in the tri-nuclear plumbate moves along the fiber axis to form the cubic **PV** structure (Fig. 3h).

The detailed analysis of 2-D XRD patterns during the conversion showed the correlation of the relative directions of the crystallographic axes of the plumbate intermediates (**INT-3** or **INT-7**) and **PV**. Fig. 3a shows the 2-D XRD pattern of multiple fibers of **INT-3** coated with MAI placed perpendicular to the horizontal line. Diffraction spots of (0*kl*) were aligned parallel to the horizontal line, indicating that the fiber axis and the crystallographic *a*-axis are together aligned vertical against the horizontal line. Fig. 3b shows the XRD pattern of the fibrous **PV** obtained by heating the fibers. Six diffraction spots on the cubic (100) circle were observed, meaning that two of the crystallographic axes of the cubic perovskite unit cell were 45° inclined against the initial crystallographic *a*-axis of **INT-3**, while the other parallel to the horizontal line. A similar correlation was observed for the conversion of **INT-7** to **PV**, with one important difference, which is reflected in the additional two diffraction spots in Fig. 3f, which indicates that there are two crystallographic directions of the resulting perovskite unit cell, one being the same as **INT-3** to **PV** conversion, the other 90° inclined along the fiber axis. Given the fact that **PV** is in equilibrium with **INT-7**, this is explained by fast inter-conversion during heating that reverts **PV** back to **INT-7** with its fiber axis either perpendicular or parallel to the initial fiber orientation. This fast conversion is also supported by remaining orientation of **INT-3** reverted from **PV** (Fig. 3c) and the lower temperature required for the full conversion of **INT-7** compared to **INT-3** in the same heating rate (Fig. i–l); the full conversion occurred at 130 °C for DMSO system while 100 °C for DMF system. In DMSO system

there were two additional intermediates (**INT-4**, **5**) characterized as MAI adduct of **INT-3** with partially removed DMSO solvate molecules.

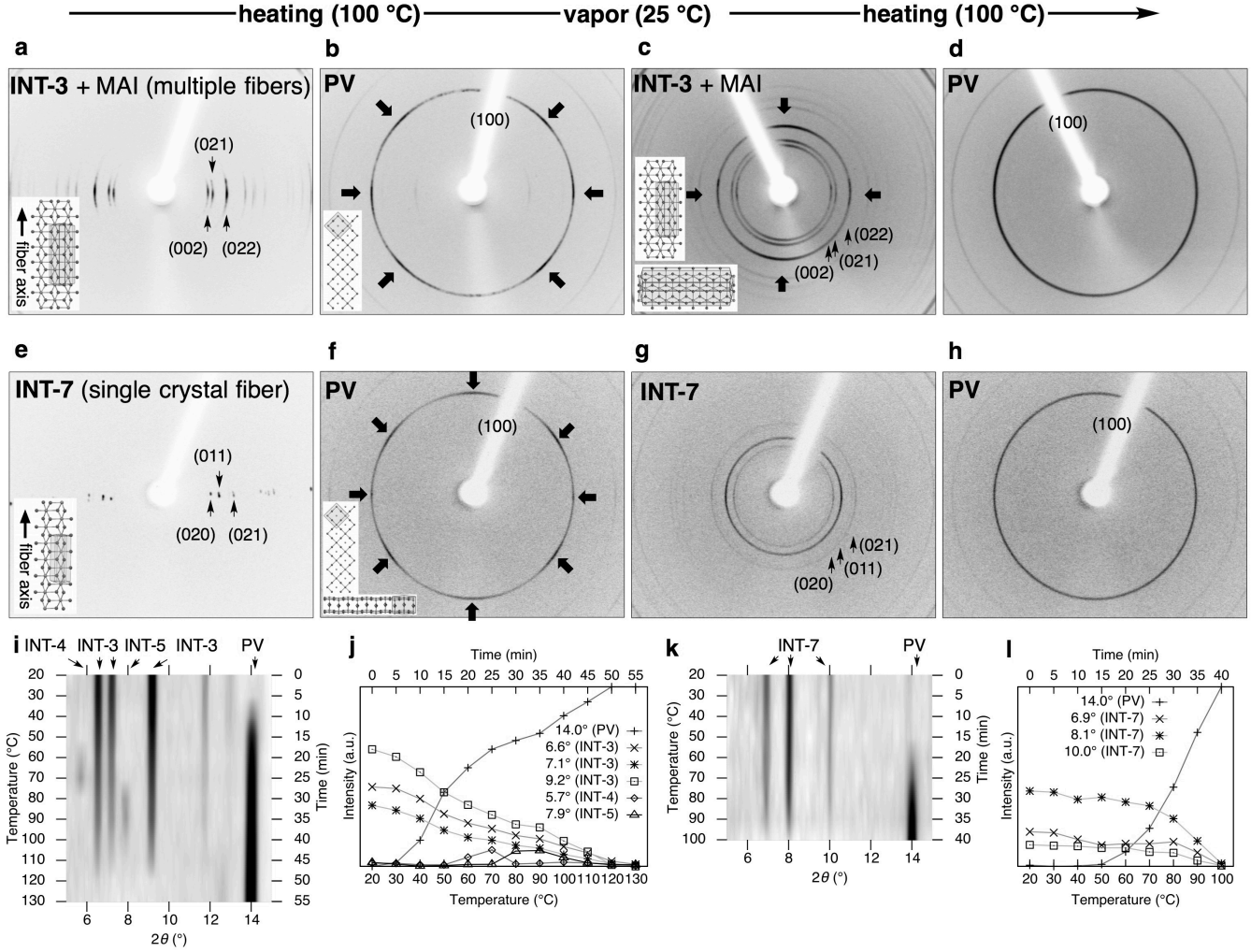

Figure 3. 2-D XRD images during the conversion between intermediates (**INT-3** or **INT-7**) and **PV** and the time course of 1-D XRD pattern. (a) **INT-3** fiber before heating. (b) After conversion to **PV**. (c) **INT-3** obtained by exposure of **PV** to DMSO vapor. (d) **PV** obtained by second heating. (e)–(h) Corresponding images in DMF system. (i) The time course of the conversion of **INT-3** to **PV**. (j) Intensity plot of Fig. 3i. (k), (l) The same set of data as Fig. 3i,j obtained for DMF system.

3. Conclusion

As an example of material formatting process, the chemical reactions that lead to **PV** were investigated through *in situ* XRD analyses. The whole chemical process of a system comprises **PI**, MAI and solvent was found to be in equilibrium. The kinetics study showed that inter-conversions even takes place during the forward process of intermediates to **PV**, depending on the solvent system. The data presented here will help rationalize the fabrication processes of perovskite solar cells and other opt-electronic devices. In addition to this, the concepts and techniques used in this study would give further implications on the study of crystal formation processes of other crystalline or functional materials.